Heliyon 10 (2024) e37917

Contents lists available at ScienceDirect

Heliyon

journal homepage: www.cell.com/heliyon

Research article

Anticancer effects of high-dose extracellular citrate treatment in pancreatic cancer cells under different glucose concentrations

Wonjin Kim [a,1], Sanghee Park [a,1], Taehyun Park [a], Seunghwan Kim [a], Jimin Kim [a], Ji-Hong Bong [a,b], Misu Lee [a,b,*]

[a] Division of Life Sciences, College of Life Science and Bioengineering, Incheon National University, Incheon, 22012, Republic of Korea
[b] Institute for New Drug Development, College of Life Science and Bioengineering, Incheon National University, 22012, Republic of Korea

ARTICLE INFO

Keywords:
Pancreatic ductal adenocarcinoma
Sodium citrate
Glucose
Extracellular citrate
Synergistic anticancer effect

ABSTRACT

Pancreatic ductal adenocarcinoma (PDAC) is a highly aggressive solid tumor. Recently, the uptake of extracellular citrate by the sodium-dependent citrate transporter (NaCT), encoded by *SLC13A5*, has been demonstrated to exert profound effects on cancer cell metabolism. However, research on the function of extracellular citrate in PDAC pathogenesis and the relationship between NaCT expression and the tumor metabolic microenvironment is limited. Therefore, we aimed to evaluate the expression of citrate transporters across a spectrum of glucose concentrations in pancreatic cancer and systematically explore the effects of sodium citrate treatment on pancreatic cancer cells at different glucose concentrations. We observed a positive correlation between glucose concentration and NaCT expression in PDAC cell lines. Extracellular sodium citrate significantly reduced cell viability partially due to reduction in intracellular Ca^{2+} levels and decreased the migration of human PDAC cells. Furthermore, we observed a decrease in the levels of the stem cell marker prominin I (CD133) following sodium citrate treatment. Notably, the combination treatment of gemcitabine and extracellular sodium citrate exhibited a synergistic anticancer effect in both two-dimensional (2D) and three-dimensional (3D) culture systems. Additionally, we confirmed that pH slightly increased upon administration of sodium citrate, indicating that this could potentially augment the efficacy of gemcitabine. Altogether, these findings suggest that exogenous sodium citrate treatment, particularly in combination with gemcitabine, may represent a novel therapeutic strategy for treating PDAC. This approach holds promise for disrupting PDAC cell metabolism and inhibiting tumor progression.

1. Introduction

Pancreatic ductal adenocarcinoma (PDAC), an aggressive solid tumor, is the fourth leading cause of global cancer-related deaths [1, 2]. Despite the introduction of innovative therapeutic strategies, PDAC prognosis remains poor, with a 5-year survival rate of less than 5 % and a median survival duration of approximately 6 months [3]. Surgical resection is often not viable for advanced PDAC; therefore, gemcitabine (genotoxic DNA-damaging agent) is the primary treatment option. However, gemcitabine often elicits a transient, minimal, or no response in most patients with unresectable PDAC, leading to therapeutic resistance, metastatic progression, and increased

* Corresponding author. Incheon National University, Incheon, Republic of Korea.
E-mail address: misulee@inu.ac.kr (M. Lee).
[1] These authors contributed equally to this work.

https://doi.org/10.1016/j.heliyon.2024.e37917
Received 2 June 2024; Received in revised form 11 September 2024; Accepted 12 September 2024
Available online 13 September 2024

mortality [4,5]. The limited efficacy of chemotherapy in patients with PDAC may be attributed to the inherent cellular diversity within the tumor microenvironment [6]. Therefore, there is an urgent need to investigate the cellular and molecular mechanisms underlying gemcitabine resistance in PDAC.

Extracellular citrate uptake and utilization play a crucial role in cancer biology. Citrate is biosynthesized within the mitochondria via the Krebs cycle from the condensation of acetyl-coenzyme A (CoA) and oxaloacetate [7]. During periods of energy surplus, citrate is exported from the mitochondria to the cytoplasm through solute carrier family member 1 (SLC25A1), also known as the citrate transporter, encoded by *SLC25A1* [8,9]. Within the cytoplasm, ATP-citrate lyase (ACLY) facilitates the breakdown of cytoplasmic citrate into acetyl-CoA, which is a pivotal building block for lipid and cholesterol synthesis [10]. Extracellular citrate is transported by the solute carrier family 13 member 5 (SLC13A5), also known as the sodium-dependent citrate transporter (NaCT), encoded by *SLC13A5*. This extracellular citrate uptake significantly affects various physiological processes and cancer cell metabolism [11,12].

An increased cytosolic citrate concentration inhibits the growth of human lung and hepatocellular carcinoma cells [13,14]. Cellular diversity within the tumor microenvironment affects tumor nutrient uptake [15]. In addition, nutrient heterogeneity is associated with anticancer agent resistance or sensitivity. Fluctuations in glucose uptake have been extensively documented to be intricately associated with variations in the responsiveness of cancer cells to a range of anticancer drugs. However, research on the function of extracellular citrate in PDAC pathogenesis and the relationship between SLC13A5 expression and the tumor metabolic microenvironment is limited.

In this study, we aimed to evaluate the expression of citrate transporters across a spectrum of glucose concentrations in pancreatic cancer. We systematically explored the effects of sodium citrate treatment on pancreatic cancer cells at different glucose concentrations. Using comprehensive two-dimensional (2D) and three-dimensional (3D) cell culture experiments, we aimed to determine the impact of high sodium citrate concentrations on tumor growth, migration, and the expression of cancer stem cell markers. To determine the clinical relevance of citrate treatment, we assessed the expression of SLC13A5 in human tissue samples.

2. Material and methods

2.1. Chemicals

Sodium citrate, D-(+)-Glucose, and gemcitabine were purchased from Sigma-Aldrich (St. Louis, MO, USA). Sodium citrate and D-(+)-glucose were dissolved in distilled water and stored at −20 °C. Gemcitabine was dissolved in distilled water to create a 1 M stock solution, which was stored at room temperature.

2.2. Cell culture

The human PDAC cell lines, MIA PaCa-2 and PANC-1, were obtained from the Korean Cell Line Bank (KCLB, Seoul, Korea). MIA PaCa-2 and PANC-1 cells were cultured in Dulbecco's modified Eagle medium (DMEM; Gibco; Thermo Fisher Scientific, Waltham, MA, USA), supplemented with 10 % fetal bovine serum (FBS; HyClone, Logan, UT, USA) and 1 % penicillin-streptomycin (Gibco; Thermo Fisher Scientific). The cells were maintained in an incubator at 37 °C with 5 % CO_2. Mycoplasma contamination was tested every 2 months. Following treatment with sodium citrate, PANC-1 and MIA PaCa-2 cells were washed with 1 × phosphate-buffered saline (PBS) and incubated with DMEM containing 1, 5, or 25 mM glucose. Media with varying concentrations of glucose were prepared by adding glucose to glucose-free DMEM to attain the desired final glucose concentration. Three-dimensional spheroids were generated from MIA PaCa-2 cells using costar ultra-low attachment multiple-well plates (Corning, Darmstadt, Germany). Cells (5000 cells/well) were plated and centrifuged at 179×*g* for 1 min. Following incubation for 2–3 days, the spheroids were visualized using phase-contrast microscopy.

2.3. Measurement of cell viability and spheroid size

MIA PaCa-2 cells (1×10^3 cells/well) were plated and incubated with 0, 1 or 10 mM sodium citrate in the presence of 1, 5, or 25 mM glucose for 48 h. Media with varying concentrations of glucose were prepared by adding glucose to glucose-free DMEM to attain the desired final glucose concentration. Cell viability was assessed using the Cell Counting Kit-8 (CCK-8; DOJINDO Laboratories, Kumamoto, Japan) according to the manufacturer's instructions. For spheroid treatment, MIA PaCa-2 cells (5000 cells/well) were premixed with 0 or 10 mM sodium citrate and 1, 5, or 25 mM glucose, followed by centrifugation at 179×*g* for 1 min. After 1 week, the spheroids were observed using an Olympus BX53 microscope (Olympus, Tokyo, Japan) and images were analyzed using Olympus CellSens software (Olympus).

2.4. Western blotting

Western blotting was performed as previously described [16]. MIA PaCa-2 and PANC-1 cells were treated with different concentrations of glucose for 8 h. MIA PaCa-2 cells were incubated with 0, 1, or 10 mM sodium citrate in media containing different glucose concentrations. Media with varying concentrations of glucose were prepared by adding glucose to glucose-free DMEM to attain the desired final glucose concentration. Following incubation, total protein was extracted using sodium dodecyl sulfate (SDS) lysis buffer, containing 1 % SDS and 60 mM Tris-HCl supplemented with a protease inhibitor (Roche, Basel, Switzerland) and phosphatase inhibitor (GenDEPOT, Katy, TX, USA). The primary antibodies used included anti-NaCT (Santa Cruz Biotechnology, Dallas, TX, USA), anti-SLC25A1 (NOVUS, Littleton, CO, USA), anti-HK2 (Abcam, Cambridge, UK), anti-CD133 (Abcam) and β-actin-HRP (Santa Cruz

Biotechnology). Details of the antibodies are summarized in Supplementary Table 1. Chemiluminescent signals were visualized using a ChemiDoc XRS system (Bio-Rad, Hercules, CA, USA). The experiments were performed in triplicate. Band quantification was conducted using ImageJ (National Institutes of Health, Bethesda, MD, USA) and Bio-Rad Image Lab 6 software (Bio-Rad).

2.5. Immunostaining

The MIA PaCa-2 cells were plated onto poly-L-lysine-coated coverslips and incubated for 24 h. Following incubation, the cells were treated with 0, or 10 mM sodium citrate at various glucose concentrations (1, 5, or 25 mM) in a glucose-free medium and incubated for an additional 24 h. Next, the cells were washed with 1 × PBS and fixed with 4 % paraformaldehyde for 20 min. After fixation, the cells were washed with 3 × PBS and blocked with 3 % bovine serum albumin for 30 min at room temperature. Subsequently, the cells were stained with Ki67 antibody (M7240, MIB-1; Agilent Technologies, Santa Clara, CA, USA). The tissue microarray comprised eight tumor regions from patients with PDAC and eight normal pancreatic regions (TissueArray.Com LLC, Derwood, USA). The primary antibody SLC13A5 (Santa Cruz, 1:500) was used for staining. Immunostaining of paraffin-embedded tissues was performed as previously described [16]. Images were acquired using an Olympus BX53 microscope (Olympus), and positive tumor regions were quantified using Olympus cellSens software (Olympus).

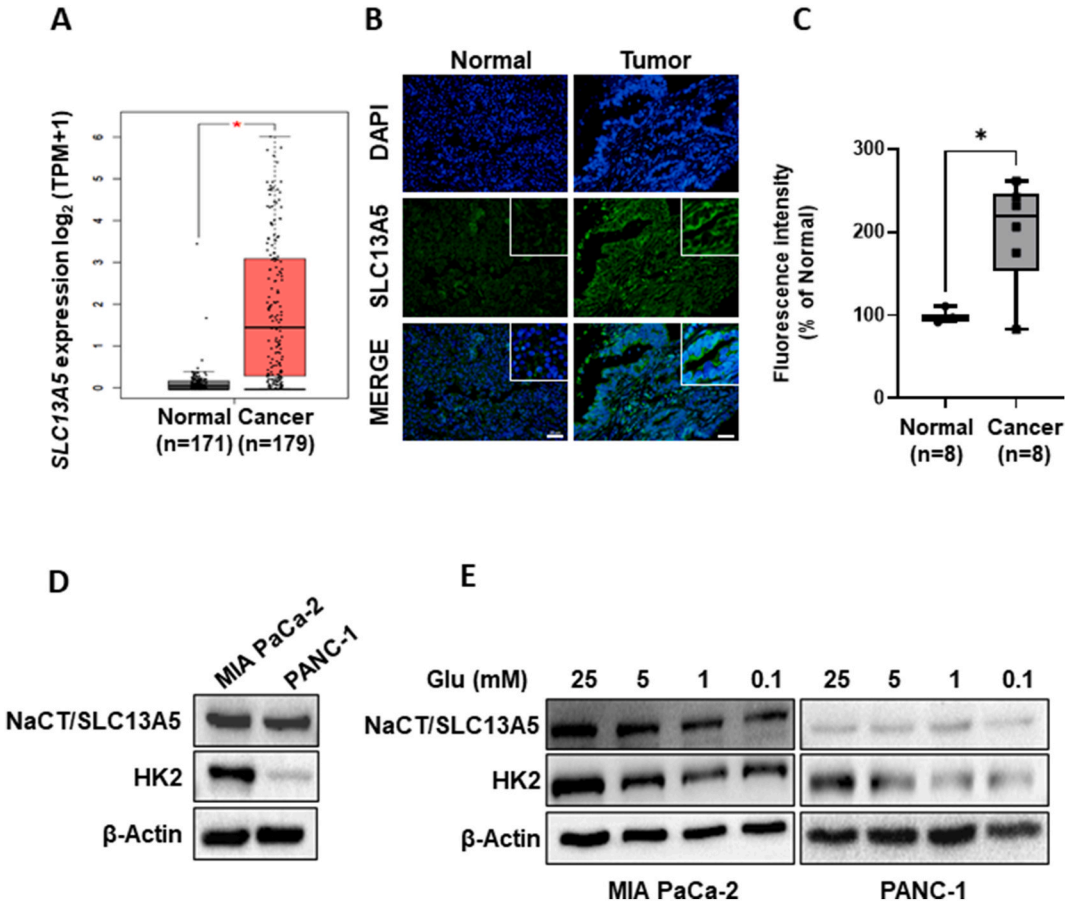

Fig. 1. Expression of NaCT/SLC13A5 in patients with pancreatic cancer. (A) The expression of *SLC13A5* in normal pancreases tissue (n = 171) and pancreatic cancer tissue (n = 179) in TCGA dataset of pancreatic cancer patients. *p < 0.05 (B) Formalin-fixed, paraffin-embedded-pancreatic cancer tissue arrays from patients with pancreatic cancer were used. Immunofluorescence was conducted using SLC13A5 (green) antibody. Counterstaining was conducted using DAPI. Scale bars: 50 μm. (B) The intensity of SLC13A5 in tumor regions from patients with pancreatic cancer (n = 8) and normal pancreatic tissue (n = 8). *p < 0.05. (C) The expression of NaCT/SLC13A5, SLC25A1, HK2, and β-actin in PANC-1 and MIA PaCa-2 cells. The quantification of band intensities from three independent experiments is shown in Supplementary Fig. 5. (D) The expression of NaCT/SLC13A5, SLC25A1, HK2, and β-actin in PANC-1 and MIA PaCa-2 cells after incubation with various concentrations of glucose (Glu) for 8 h. The quantification of band intensities from three independent experiments is shown in Supplementary Fig. 6. NaCT, sodium-dependent citrate transporter; SLC13A5, solute carrier family 13 member 5; DAPI, 4′,6-diamidino-2-phenylindole; TCGA, The Cancer Genome Atlas; SLC25A1, solute carrier family 25 member 1; HK2, hexokinase 2; PANC-1 and MIA PaCa-2, pancreatic cancer cell lines.

2.6. Scratch wound-healing assay and migration assay

For the scratch wound-healing assay, MIA PaCa-2 cells were cultured in 12-well plates until 100 % confluency was reached. A pipette tip was used to create wounds, and the medium was replaced with a treatment medium containing 0.1 % serum to inhibit cell proliferation. Migration assays were performed using 24-multiwell uncoated polycarbonate membrane inserts (BioCoat; BD Biosciences, Heidelberg, Germany). MIA PaCa-2 cells were treated according to the specified conditions. After 24 h, the cells were trypsinized, suspended in 0.1 % FBS, and added to the upper chamber of the insert (50,000 cells/well). The chamber was filled with medium containing 10 % FBS. The cells were incubated for 24 h to allow migration through the membrane. Following incubation, the migrated cells were fixed in 100 % methanol and stained with a 1.5 % (w/v) toluidine blue solution in water. Images were captured using an Olympus BX53 microscope with Olympus CellSens software (Olympus).

2.7. Measurements of intracellular Ca^{2+} and pH level

To detect intracellular Ca^{2+}, MIA PaCa-2 and PANC-1 cells were incubated with 5 μM of Fluo-4 AM (Invitrogen, Waltham, MA, USA) fluorescent indicator for 1 h after treatment with a high concentration of sodium citrate. After incubation, the cells were washed with PBS. The intracellular Ca^{2+} levels were determined by measuring the fluorescence intensity of Fluo-4 AM using a fluorescence plate reader (Promega, Madison, WI, USA). To measure intracellular pH, MIA PaCa-2 and PANC-1 cells were treated with a high concentration of sodium citrate for 24 h and then incubated with the pHrodo™ Red AM Intracellular pH Indicator Dye system (Thermo Fisher Scientific). Intracellular pH measurements were performed as previously described [17].

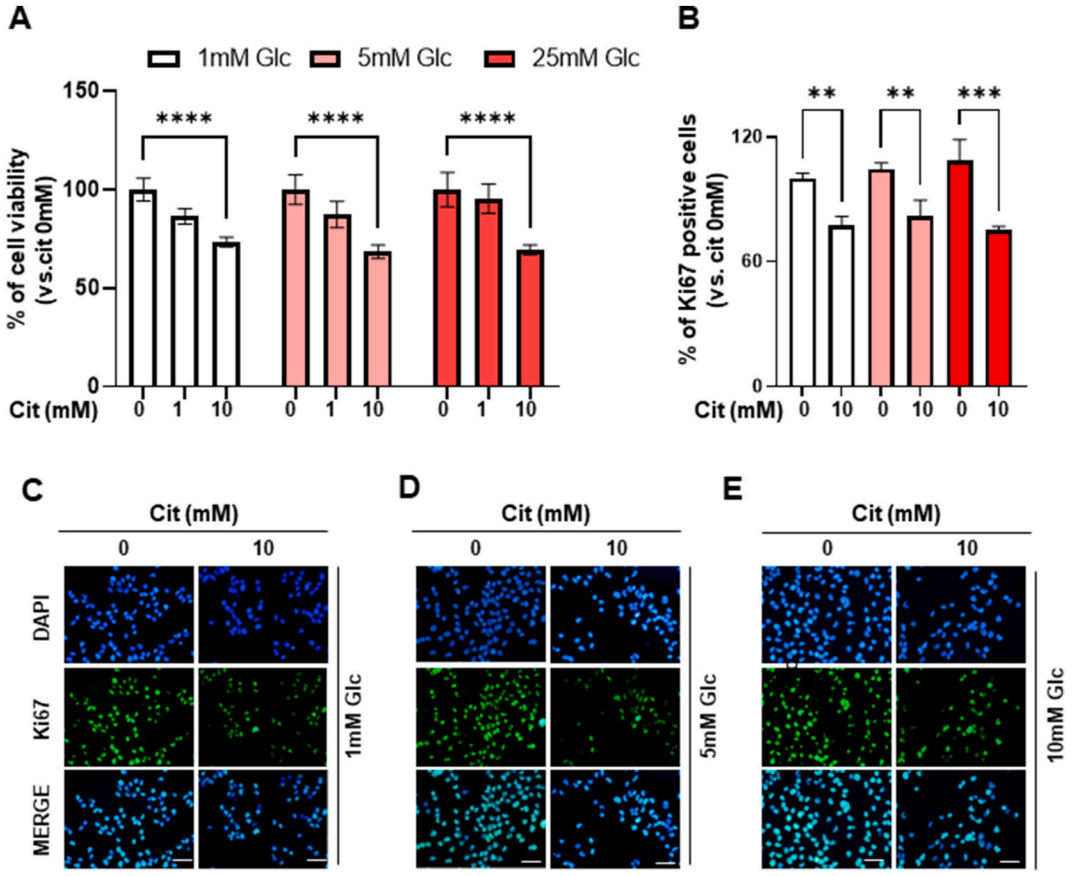

Fig. 2. Inhibition of cell proliferation after citrate treatment. (A) Cell viability in MIA CaPa-2 cells following 0, 1, or 10 mM sodium citrate treatment in media with varying glucose concentrations for 48 h. The experiment was performed in triplicate with multiple replicates. Results are presented as the mean ± SD; ****$p < 0.0001$ (B) The percentage of Ki67-positive cells after 0 or 10 mM sodium citrate treatment in a medium with various glucose concentrations for 48 h. Six random fields were quantified for each independent test ($n = 3$) at × 200 magnification, and the results are presented as the mean ± SD; **$p < 0.01$; ***$p < 0.001$ (C–E) Representative immunocytochemistry of Ki67 in MIA PaCa-2 cells after 0 or 10 mM citrate treatment in medium containing 1 mM (C), 5 mM (D), and 25 mM (E) glucose for 48 h. Scale bar: 50 μm. MIA CaPa-2, a pancreatic cancer cell line; SD, standard deviation.

2.8. Statistical analysis

Statistical analyses were conducted using GraphPad Prism software (GraphPad Software Inc., San Diego, CA, USA). Differences among three or more groups were analyzed using one-way analysis of variance (ANOVA) followed by Tukey's multiple comparison test. A paired two-tailed Student's t-test was used to analyze differences between the two datasets. Statistical significance was set at $p < 0.05$.

3. Results

3.1. Expression of SLC13A5 in patients with pancreatic cancer

We examined the expression of SLC13A5 in patients with pancreatic cancer. Analysis of data from The Cancer Genome Atlas

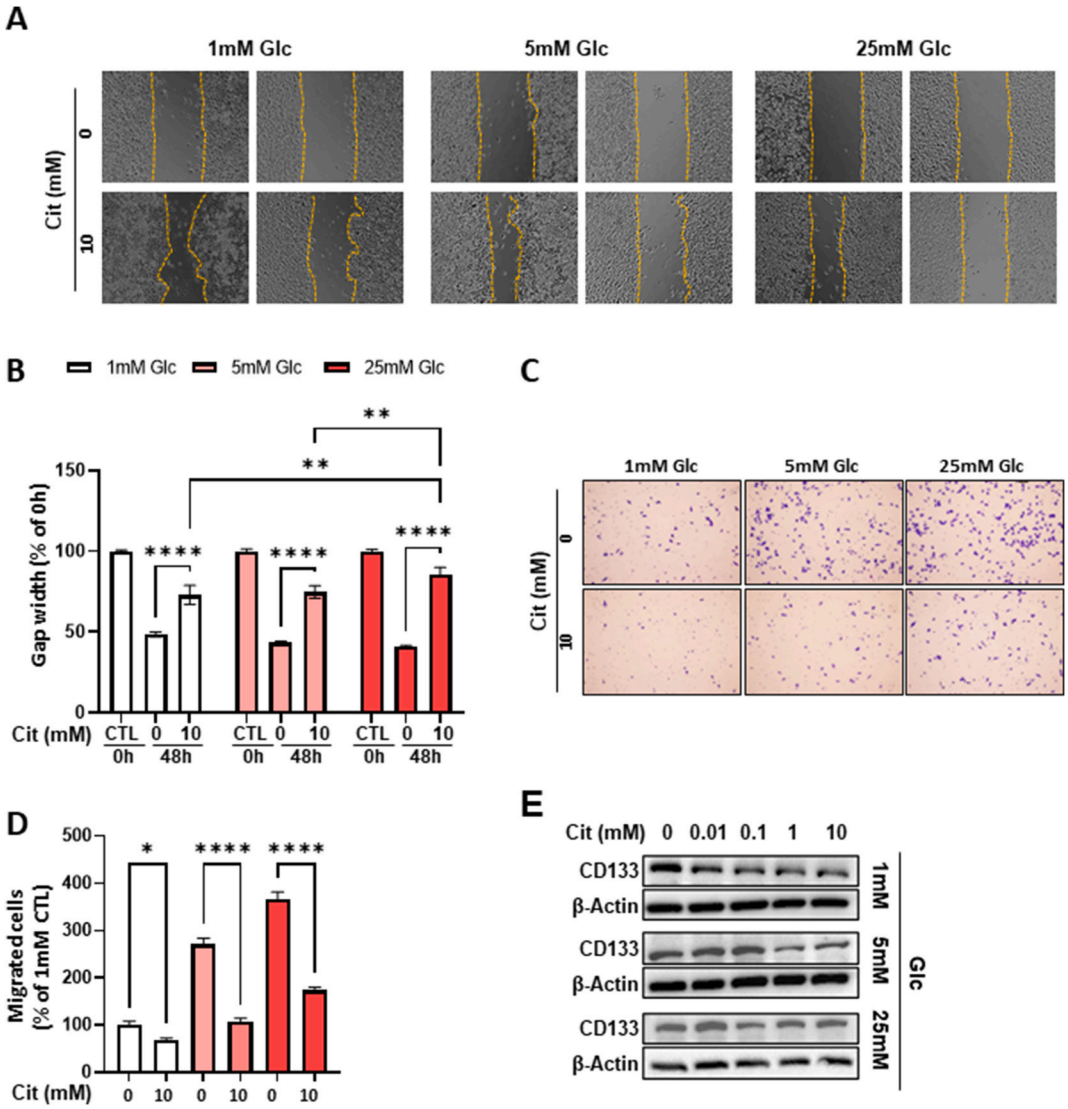

Fig. 3. Inhibition of cell migration and CD133 expression after treatment with extracellular sodium citrate. (A) A scratch wound-healing assay was conducted on MIA PaCa-2 cells. Cell migration was monitored by inverted microscopy at 0 and 48 h after treatment with 0 or 10 mM sodium citrate in a medium with various concentrations of glucose. (B) The percentage of gap width of (A). (C) Migration assay using MIA PaCa-2 cells treated with various concentrations of sodium citrate and glucose for 24 h. The experiment was independently performed in triplicate. (D) Quantification of migrated cells of (C). Data are expressed as the mean ± SD. Five random fields of each test (n = 3) at × 200 magnification were counted. *$p < 0.05$; ****$p < 0.0001$. (E) CD133 and β-actin expression levels in MIA PaCa-2 cells after treatment under the indicated conditions for 24 h. The quantification of band intensities from three independent experiments is shown in Supplementary Fig. 7. MIA PaCa-2, a pancreatic cancer cell line; SD, standard deviation; CD133, prominin I, a cell-surface antigen.

(TCGA) analysis using GEPIA (Gene Expression Profiling Interactive Analysis, http://gepia.cancer-pku.cn/) revealed that *SLC13A5* expression is higher in patients with pancreatic cancer (n = 179) compared to healthy individuals (n = 171; Fig. 1A). Additionally, using a pancreatic cancer tissue array, we confirmed that membranous expression of SLC13A5 was significantly higher in tumor regions (n = 8) in patients with PDAC compared to normal pancreatic tissue (n = 8, Fig. 1B and C). Despite the limited sample size, these findings indicate that patients with pancreatic cancer exhibit higher expression levels of SLC13A5 at both RNA and protein levels. Consequently, high concentrations of sodium citrate may exert a beneficial anticancer effect.

3.2. Citrate transporter expression is glucose-dependent

The PANC-1 and MIA PaCa-2 cell lines are commonly employed as *in vitro* models for studying PDAC. Both cell types demonstrated the expression of SLC13A5, a plasma citrate transporter, and SLC25A1, a mitochondrial citrate carrier. Notably, both SLC25A1 and SLC13A5 exhibited higher expression levels in MIA PaCa-2 cells (Fig. 1C). We found that increased glucose levels led to elevated SLC13A5 expression, whereas that of SLC25A1 remained relatively unchanged (Fig. 1D). Further analysis of data from TCGA involving patients with pancreatic cancer (n = 173) revealed a positive correlation between *SLC2A1* and *SLC13A5* expression (p = 0.0002; Supplementary Fig. 1A). No correlation was found between *SLC25A1* and *SLC2A1* expression (p = 0.2319; Supplementary Fig. 1B). These findings demonstrate that the glycolytic microenvironment influences SLC13A5 expression in PDAC cells. Based on these findings, we focused our subsequent experiments on the role of SLC13A5 in pancreatic cancer.

3.3. Extracellular citrate treatment negatively influences cancer cell proliferation

We conducted further experiments on MIA PaCa-2 cells, which are characterized by high expression levels of NaCT and hexokinase 2 (HK2). To determine the effect of citrate utilization under different glucose concentrations, we evaluated the proliferation rate of cells treated with sodium citrate under varying glucose conditions. High-concentration sodium citrate treatment decreased MIA PaCa-2 cell proliferation, regardless of glucose concentration (Fig. 2A). Additionally, sodium citrate treatment decreased the percentage of Ki67-positive cells (1 mM Glu; −22.5 %, 5 mM Glu; −18 %, 25 mM Glu; −25 %, Fig. 2B–E). To elucidate the mechanisms underlying the anticancer effect of high concentrations of extracellular sodium citrate, we measured intracellular Ca^{2+} concentration to determine whether sodium citrate functions as a Ca^{2+} chelator. Intracellular Ca^{2+} levels were significantly reduced by 28.5 % in MIA PaCa-2 cells (Supplementary Fig. 2A), suggesting that the decrease in cell viability may be partly due to decreased intracellular Ca^{2+} levels.

Furthermore, we examined the effect of citrate on cell migration using both cell scratch wound-healing and migration chamber assays. In the cell scratch wound-healing assay, the sodium citrate-treated cells failed bridge and repair the cell-free region, suggesting reduced migration after sodium citrate treatment (Fig. 3A and B). In the migration chamber assay, a significant reduction in the number of migrating cells was observed after citrate treatment (Fig. 3C and D). Elevated CD133 expression is closely linked to tumor development and serves as a marker of cancer stem cells in various types of cancer, including pancreatic cancer. Notably, we observed a decrease in CD133 levels after citrate treatment, suggesting a potential reduction in cancer stem cells (Fig. 3E). In summary, a high concentration of citrate inhibited the proliferation and migration of PDAC cells. Additionally, glucose did not significantly influence the cellular effects of citrate.

3.4. Exogenous citrate exhibits anticancer effects

To confirm the anticancer effects of citrate on PDAC cells, we developed 3D spheroids using MIA PaCa-2 cells. Increased glucose levels induced an increase in spheroid size. Consistent with the results observed in the 2D culture system, citrate treatment significantly reduced spheroid size by approximately 30 %. However, in contrast to the 2D system, glucose influenced spheroid reduction; 25 mM glucose had a greater impact on spheroid reduction than 1 mM and 5 mM glucose (Fig. 4A and B). These results suggest that the

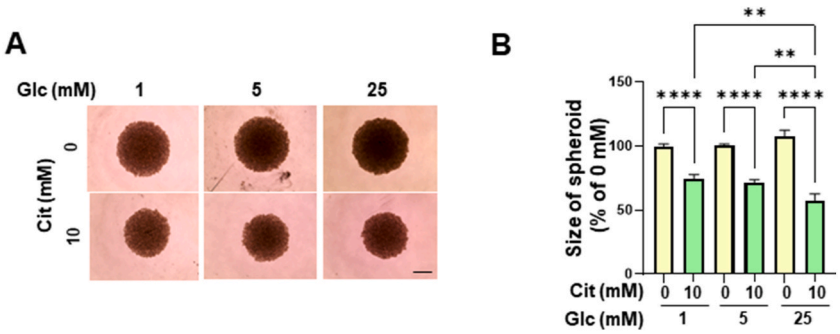

Fig. 4. Reduction in MIA PaCa-2 cell-derived spheroids. (A) Spheroids after treatment with 0 or 10 mM sodium citrate in medium with the indicated glucose concentrations for 72 h, analyzed using an inverted microscope. Scale bar: 100 μm (B) The relative change in spheroid size (n = 3 in each of the three independent experiments) was estimated using Olympus CellSens software. The data are expressed as the mean ± SD. **p < 0.01. MIA PaCa-2, a pancreatic cancer cell line; SD, standard deviation.

anticancer effect of citrate treatment is enhanced in high-glucose environments.

3.5. Synergic anticancer effect of citrate and gemcitabine

Although citrate treatment alone has an anticancer effect, we explored the potential synergistic anticancer effects of combining citrate with gemcitabine, an established first-line treatment for patients with advanced pancreatic cancer. The combination treatment resulted in significantly lower cell viability than that after single treatment in both MIA PaCa-2 and PANC-1 cells (Fig. 5A and Supplementary Fig. 3A). In the 3D spheroid model, combination treatment significantly reduced spheroid size, with a greater reduction observed compared with the single treatment (Fig. 5B and C; Supplementary Figs. 3B and C). Notably, the anticancer effect was more pronounced in the 3D spheroid system than in the 2D system. Furthermore, the number of migrated cells was significantly lower following combination treatment compared to the single treatment (Fig. 5D and E; Supplementary Figs. 3D and E). These results indicate a synergistic effect rather than an additive anticancer effect. This synergetic effect was quantified and is presented in Supplementary Table 2. Overall, combination of citrate and gemcitabine demonstrated a more pronounced anticancer effect in both 2D and 3D culture systems compared to the single treatment.

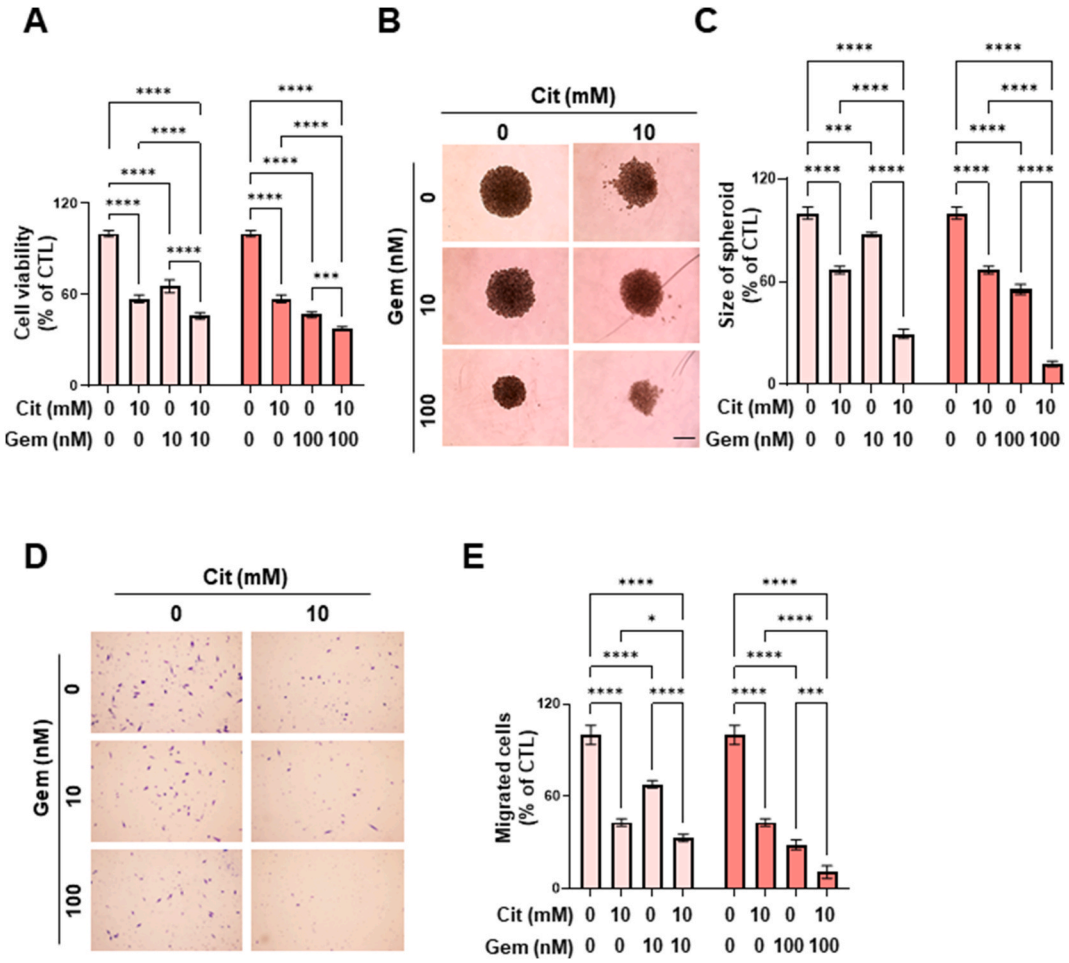

Fig. 5. Synergic anticancer effect of sodium citrate and gemcitabine. (A) Cell viability in MIA CaPa-2 cells following treatment with 0 or 10 mM sodium citrate and 0, 10, or 100 nM gemcitabine. The experiment was conducted in triplicate with multiple replicates. Results are presented as the mean ± SD; ***$p < 0.001$, ****$p < 0.0001$. (B) Representative spheroids after treatment with 0 or 10 mM sodium citrate and 0, 10, or 100 nM gemcitabine for 72 h, analyzed using an inverted microscope. Scale bar: 100 μm. (C) The relative change in spheroid size (n = 3 in each of the three independent experiments) was estimated using Olympus CellSens software. Data are presented as the mean ± SD. ***$p < 0.001$, ****$p < 0.0001$. (D) Migration assay using MIA PaCa-2 cells treated with 0 or 10 mM sodium citrate and 0, 10, or 100 nM gemcitabine for 24 h. The experiment was independently performed in a triplicate. (E) Quantification of migrated cells of (D). The data are expressed as the mean ± SD. *$p < 0.05$, ***$p < 0.001$, ****$p < 0.0001$. MIA CaPa-2, a pancreatic cancer cell line; SD, standard deviation.

4. Discussion

Cancer cells take up a variety of nutrients and metabolites from their extracellular microenvironment, each playing specific roles in cellular functions [18]. Citrate, derived from mitochondrial synthesis or α-ketoglutarate carboxylation, is cleaved by ACLY into acetyl-CoA and oxaloacetate [7]. This process is essential for fatty acid synthesis and cell growth, making citrate a key player in cancer metabolism and regulation [19]. The rapid consumption and turnover of these molecules in highly proliferative cancer cells leads to a constantly low citrate concentration, which may prevent the retroactive inhibition of glycolytic enzymes. There is limited research on the function of extracellular citrate in PDAC pathogenesis. Therefore, we aimed to determine the effect of extracellular citrate treatment on PDAC cells with varying glucose concentrations. Additionally, we investigated the synergistic anticancer effect of sodium citrate and gemcitabine.

Studies on the utilization of extracellular citrate by cancer cells remain controversial, with low citrate concentrations potentially promoting cell proliferation, while higher concentrations exhibit anticancer properties [20,21]. Kumar et al. demonstrated that treating hypoxic liver cancer cells with low concentrations of citrate (<1 mM) resulted in increased metabolism of extracellular citrate into fatty acids and TCA intermediates [22]. Drexler et al. showed that extracellular citrate (200–300 μM) enhances the metastatic activity and therapeutic resistance of cancer cells [23]. Also, inhibiting citrate import by silencing *SLC13A5* reduces tumor growth and metastasis, likely owing to the central role of citrate in fatty acid synthesis [12]. Conversely, recent studies have indicated that treatment with high concentrations of extracellular citrate inhibits cancer cell growth [13,14,24,25]. Our group also demonstrated that sodium citrate (>1 mM) inhibits liver cancer cell growth by reducing glucose uptake and inducing hypoxia inducible factor 1 subunit alpha degradation [14]. Petillo et al. observed decreased lipid deposition, reduced histone acetylation, and inhibition of ACLY activity in the presence of 15 mM sodium citrate [20]. Additionally, Wu et al. found that sodium citrate decreased Ca^{2+} levels and inhibited the glycolysis pathway, resulting in induced cell apoptosis in ovarian cancer cells [25]. Moreover, oral citrate administration induces antitumor effects in patients with cancer [26,27]. The results from these previous studies are consistent with our findings, showing reduced PDAC cell proliferation and migration with high-concentration citrate treatment. Thus, the dual role of citrate—promoting cancer at low concentrations and inhibiting it at high concentrations—depends on the cellular context and citrate levels. Prostate cancer research highlights this duality. The prostate gland primarily produces and releases high levels of citrate (up to 180 mM) into the prostatic fluid, serving as an energy source for sperm. However, citrate levels significantly decrease in prostate cancer, particularly in metastatic disease, thereby potentially influencing tumor metabolism and progression.

We investigated the expression of SLC13A5 under varying glucose concentrations in pancreatic cancer cells (MIA PaCa-2 and PANC-1). Our goal was to determine whether increased glycolysis in cancer cells, which adversely affects clinical outcomes [28,29], impacts the expression of SLC13A5. The expression of SLC13A5 was increased in pancreatic cancer cells with elevated HK2 expression (a marker of glycolysis) under high glucose conditions. Therefore, our findings suggest that citrate treatment could be more effective in highly glycolytic pancreatic cancer cells due to the upregulation of SLC13A5, facilitating citrate entry into the cells. In our results, there were no significant differences in cell viability and Ki67 proliferation index, but the wound-healing and migration assays showed a slightly higher inhibitory effect after citrate treatment under 25 mM glucose conditions compared to low glucose conditions in the 2D culture system. In the 3D culture system, there was a greater decrease in spheroid size after treatment with 10 mM citrate under 25 mM glucose conditions. Therefore, sodium citrate treatment may have a more pronounced anticancer effect on glycolytic pancreatic cancer cells with high expression of SLC13A5.

To elucidate the mechanisms underlying the anticancer effect of high concentrations of extracellular sodium citrate, we measured intracellular Ca^{2+} concentration to determine whether sodium citrate functions as a Ca^{2+} chelator. Intracellular Ca^{2+} levels were significantly reduced in MIA PaCa-2 cells, whereas in PANC-1 cells, the reduction was not statistically significant. This reduction in intracellular Ca^{2+} correlated with decreased cell viability. In MIA PaCa-2 cells, treatment with 10 mM sodium citrate resulted in a 30 % reduction in cell viability (Fig. 2A), whereas in PANC-1 cells, only a 5 % reduction was observed (Supplementary Fig. 3A). These findings suggest that the reduction in cell viability may be partly due to decreased intracellular Ca^{2+} levels. Furthermore, citrate elevates pH value, thereby neutralizing the tumor microenvironment. This pH neutralization has been shown to enhance the penetration of certain anticancer drugs into cancer tissues. This has been demonstrated in an animal model of pancreatic cancer, where the penetration of 5-FU increased with citrate treatment [30]. In the present study, we observed a slight increase in pH upon administration of sodium citrate (Supplementary Fig. 4), which could potentially enhance the efficacy of gemcitabine.

Gemcitabine is the first-line chemotherapy drug for PDAC and the most widely used agent for metastatic PDAC. However, its efficacy is often limited owing to the development of chemoresistance [1]. CD133 is a recognized marker for cancer stem cells in various cancers, including pancreatic cancer, and its expression is associated with poor prognosis in these patients [31,32]. Furthermore, CD133-positive PDAC cells may serve as cancer stem cells, enhancing cell migration and invasion, thus playing a pivotal role in gemcitabine resistance [33]. In this study, we observed a decrease in CD133 levels following high-dose citrate treatment. Additionally, the combination of citrate and gemcitabine reduced cancer stem cell populations in gemcitabine-resistant PDAC. To further validate the anticancer potential of citrate, we developed 3D spheroids using MIA PaCa-2 cells. Similar to 2D culture systems, these spheroids exhibited a significant reduction in size after citrate treatment. Notably, the spheroids cultured with higher glucose concentrations showed a more pronounced size reduction following citrate treatment, indicating a potential glucose-dependent effect.

Although our study highlights the anticancer effects of high extracellular citrate concentrations, it was conducted *in vitro*, which limits the generalizability of these findings. Therefore, further *in vivo* animal experiments are needed to confirm these results. Nevertheless, the significant reduction in the size of 3D PDAC spheroids observed in this study suggests that similar anticancer effects may be observed in further *in vivo* research.

5. Conclusions

In this study, we explored the impact of citrate on PDAC and identified its concentration-dependent effects, particularly its potential for sensitizing pancreatic cancer cells to gemcitabine. These findings highlight the pivotal role of citrate as a therapeutic agent and provide valuable insights into novel strategies for treating pancreatic cancer.

Ethics approval and consent to participate

No applicable.

Consent for publication

No applicable.

Availability of data and materials

All data generated or analyzed during this study are included in this published article.

Funding

This research was supported by the National Research Foundation of Korea (grant number: NRF-2022R1A2C1007956) and by an Incheon National University Research Grant (grant number: 2024-0072).

CRediT authorship contribution statement

Wonjin Kim: Visualization, Methodology, Investigation. **Sanghee Park:** Visualization, Investigation. **Taehyun Park:** Visualization, Investigation. **Seunghwan Kim:** Validation, Investigation. **Jimin Kim:** Validation. **Ji-Hong Bong:** Validation. **Misu Lee:** Writing – original draft, Supervision, Funding acquisition, Conceptualization.

Declaration of competing interest

The authors declare there is no conflict of interests.

Acknowledgements

No applicable.

List of abbreviations

Pancreatic ductal adenocarcinoma PDAC
ATP-citrate lyase ACLY
Korean Cell Line Bank KCLB
Dulbecco's modified Eagle's medium DMEM
Fetal bovine serum FBS
Cell Counting Kit-8 CCK-8
Sodium dodecyl sulfate SDS
Phosphate-buffered saline PBS
Analysis of variance ANOVA
Insulin-like growth factor type 1 receptor IGF-1R
Eukaryotic translation initiation factor 2A eIF2A
The Cancer Genome Atlas Program TCGA
Adenosine triphosphate ATP
Tricarboxylic Acid Cycle TCA

Appendix A. Supplementary data

Supplementary data to this article can be found online at https://doi.org/10.1016/j.heliyon.2024.e37917.

References

[1] I. Garrido-Laguna, M. Hidalgo, Pancreatic cancer: from state-of-the-art treatments to promising novel therapies, Nat. Rev. Clin. Oncol. 12 (2015) 319–334.
[2] L. Rahib, M.R. Wehner, L.M. Matrisian, K.T. Nead, Estimated projection of US cancer incidence and death to 2040, JAMA Netw. Open 4 (2021) e214708.
[3] A. Vincent, J. Herman, R. Schulick, R.H. Hruban, M. Goggins, Pancreatic cancer, Lancet 378 (2011) 607–620.
[4] D.D. Von Hoff, T. Ervin, F.P. Arena, E.G. Chiorean, J. Infante, M. Moore, T. Seay, S.A. Tjulandin, W.W. Ma, M.N. Saleh, M. Harris, M. Reni, S. Dowden, D. Laheru, N. Bahary, R.K. Ramanathan, J. Tabernero, M. Hidalgo, D. Goldstein, E. Van Cutsem, X. Wei, J. Iglesias, M.F. Renschler, Increased survival in pancreatic cancer with nab-paclitaxel plus gemcitabine, N. Engl. J. Med. 369 (2013) 1691–1703.
[5] M. Amrutkar, I.P. Gladhaug, Pancreatic cancer chemoresistance to gemcitabine, Cancers 9 (2017).
[6] W.J. Ho, E.M. Jaffee, L. Zheng, The tumour microenvironment in pancreatic cancer - clinical challenges and opportunities, Nat. Rev. Clin. Oncol. 17 (2020) 527–540.
[7] M. Akram, Citric acid cycle and role of its intermediates in metabolism, Cell Biochem. Biophys. 68 (2014) 475–478.
[8] E.R.S. Kunji, M.S. King, J.J. Ruprecht, C. Thangaratnarajah, The SLC25 carrier family: important transport proteins in mitochondrial physiology and pathology, Physiology 35 (2020) 302–327.
[9] F. Palmieri, The mitochondrial transporter family SLC25: identification, properties and physiopathology, Mol. Aspect. Med. 34 (2013) 465–484.
[10] D.M. Gibson, R.T. Lyons, D.F. Scott, Y. Muto, Synthesis and degradation of the lipogenic enzymes of rat liver, Adv. Enzym. Regul. 10 (1972) 187–204.
[11] K. Inoue, L. Zhuang, V. Ganapathy, Human Na+ -coupled citrate transporter: primary structure, genomic organization, and transport function, Biochem. Biophys. Res. Commun. 299 (2002) 465–471.
[12] Z. Li, D. Li, E.Y. Choi, R. Lapidus, L. Zhang, S.M. Huang, P. Shapiro, H. Wang, Silencing of solute carrier family 13 member 5 disrupts energy homeostasis and inhibits proliferation of human hepatocarcinoma cells, J. Biol. Chem. 292 (2017) 13890–13901.
[13] J.G. Ren, P. Seth, H. Ye, K. Guo, J.I. Hanai, Z. Husain, V.P. Sukhatme, Citrate suppresses tumor growth in multiple models through inhibition of glycolysis, the tricarboxylic acid cycle and the IGF-1R pathway, Sci. Rep. 7 (2017) 4537.
[14] S.Y. Kim, D. Kim, J. Kim, H.Y. Ko, W.J. Kim, Y. Park, H.W. Lee, D.H. Han, K.S. Kim, S. Park, M. Lee, M. Yun, Extracellular citrate treatment induces HIF1alpha degradation and inhibits the growth of low-glycolytic hepatocellular carcinoma under hypoxia, Cancers 14 (2022).
[15] H. Ying, A.C. Kimmelman, C.A. Lyssiotis, S. Hua, G.C. Chu, E. Fletcher-Sananikone, J.W. Locasale, J. Son, H. Zhang, J.L. Coloff, H. Yan, W. Wang, S. Chen, A. Viale, H. Zheng, J.H. Paik, C. Lim, A.R. Guimaraes, E.S. Martin, J. Chang, A.F. Hezel, S.R. Perry, J. Hu, B. Gan, Y. Xiao, J.M. Asara, R. Weissleder, Y.A. Wang, L. Chin, L.C. Cantley, R.A. DePinho, Oncogenic Kras maintains pancreatic tumors through regulation of anabolic glucose metabolism, Cell 149 (2012) 656–670.
[16] H. Jo, Y. Park, T. Kim, J. Kim, J.S. Lee, S.Y. Kim, J.I. Chung, H.Y. Ko, J.C. Pyun, K.S. Kim, M. Lee, M. Yun, Modulation of SIRT3 expression through CDK4/6 enhances the anti-cancer effect of sorafenib in hepatocellular carcinoma cells, BMC Cancer 20 (2020) 332.
[17] J.S. Sung, Y. Han, T.G. Yun, J. Jung, T.H. Kim, F. Piccinini, M.J. Kang, J. Jose, M. Lee, J.C. Pyun, Monocarboxylate transporter-1 (MCT-1) inhibitors screened from autodisplayed F(V)-antibody library, Int. J. Biol. Macromol. 265 (2024) 130854.
[18] N.N. Pavlova, C.B. Thompson, The emerging hallmarks of cancer metabolism, Cell Metab 23 (2016) 27–47.
[19] P. Icard, L. Poulain, H. Lincet, Understanding the central role of citrate in the metabolism of cancer cells, Biochim. Biophys. Acta 1825 (2012) 111–116.
[20] A. Petillo, V. Abruzzese, P. Koshal, A. Ostuni, F. Bisaccia, Extracellular citrate is a trojan horse for cancer cells, Front. Mol. Biosci. 7 (2020) 593866.
[21] P. Icard, L. Simula, G. Zahn, M. Alifano, M.E. Mycielska, The dual role of citrate in cancer, Biochim. Biophys. Acta Rev. Canc 1878 (2023) 188987.
[22] A. Kumar, T. Cordes, A.E. Thalacker-Mercer, A.M. Pajor, A.N. Murphy, C.M. Metallo, NaCT/SLC13A5 facilitates citrate import and metabolism under nutrient-limited conditions, Cell Rep. 36 (2021) 109701.
[23] K. Drexler, K.M. Schmidt, K. Jordan, M. Federlin, V.M. Milenkovic, G. Liebisch, A. Artati, C. Schmidl, G. Madej, J. Tokarz, A. Cecil, W. Jagla, S. Haerteis, T. Aung, C. Wagner, M. Kolodziejczyk, S. Heinke, E.H. Stanton, B. Schwertner, D. Riegel, C.H. Wetzel, W. Buchalla, M. Proescholdt, C.A. Klein, M. Berneburg, H. J. Schlitt, T. Brabletz, C. Ziegler, E.K. Parkinson, A. Gaumann, E.K. Geissler, J. Adamski, S. Haferkamp, M.E. Mycielska, Cancer-associated cells release citrate to support tumour metastatic progression, Life Sci. Alliance 4 (2021).
[24] Y. Lu, X. Zhang, H. Zhang, J. Lan, G. Huang, E. Varin, H. Lincet, L. Poulain, P. Icard, Citrate induces apoptotic cell death: a promising way to treat gastric carcinoma? Anticancer Res. 31 (2011) 797–805.
[25] Y. Wu, C. Jia, W. Liu, W. Zhan, Y. Chen, J. Lu, Y. Bao, S. Wang, C. Yu, L. Zheng, L. Sun, Z. Song, Sodium citrate targeting Ca(2+)/CAMKK2 pathway exhibits anti-tumor activity through inducing apoptosis and ferroptosis in ovarian cancer, J. Adv. Res. (2024), https://doi.org/10.1016/j.jare.2024.04.033.
[26] A.H. Bucay, Clinical report: a patient with primary peritoneal mesothelioma that has improved after taking citric acid orally, Clin Res Hepatol Gastroenterol 35 (2011) 241.
[27] Bucay A. Halabe, Hypothesis proved…citric acid (citrate) does improve cancer: a case of a patient suffering from medullary thyroid cancer, Med. Hypotheses 73 (2009) 271.
[28] M. Lee, J.Y. Jeon, M.L. Neugent, J.W. Kim, M. Yun, 18F-Fluorodeoxyglucose uptake on positron emission tomography/computed tomography is associated with metastasis and epithelial-mesenchymal transition in hepatocellular carcinoma, Clin. Exp. Metastasis 34 (2017) 251–260.
[29] T. Migita, T. Narita, K. Nomura, E. Miyagi, F. Inazuka, M. Matsuura, M. Ushijima, T. Mashima, H. Seimiya, Y. Satoh, S. Okumura, K. Nakagawa, Y. Ishikawa, ATP citrate lyase: activation and therapeutic implications in non-small cell lung cancer, Cancer Res. 68 (2008) 8547–8554.
[30] H. Ando, K. Eshima, T. Ishida, Neutralization of acidic tumor microenvironment (TME) with daily oral dosing of sodium potassium citrate (K/Na citrate) increases therapeutic effect of anti-cancer agent in pancreatic cancer xenograft mice model, Biol. Pharm. Bull. 44 (2021) 266–270.
[31] S. Chen, X. Song, Z. Chen, X. Li, M. Li, H. Liu, J. Li, CD133 expression and the prognosis of colorectal cancer: a systematic review and meta-analysis, PLoS One 8 (2013) e56380.
[32] A. Nomura, S. Banerjee, R. Chugh, V. Dudeja, M. Yamamoto, S.M. Vickers, A.K. Saluja, CD133 initiates tumors, induces epithelial-mesenchymal transition and increases metastasis in pancreatic cancer, Oncotarget 6 (2015) 8313–8322.
[33] P.C. Hermann, S.L. Huber, T. Herrler, A. Aicher, J.W. Ellwart, M. Guba, C.J. Bruns, C. Heeschen, Distinct populations of cancer stem cells determine tumor growth and metastatic activity in human pancreatic cancer, Cell Stem Cell 1 (2007) 313–323.